IFAC Conference on Advances in PID Control
PID'12
Brescia (Italy), March 28-30, 2012 FrPS.2

A New Methodology to Design Sliding-PID Controllers: Application to Missile Flight Control System

B. Kada*

**Aeronautical Engineering Department, King Abdulaziz University, P.O. Box 80204, Jeddah, 21589 KSA (Tel: 966-2-640-2000 ext. 68729; e-mail: bkada@kau.edu.sa).*

Abstract: In this paper, a new methodology to design robust sliding-PID tracking motion controllers for a certain class of nonlinear systems is presented. The methodology is based upon the combination of the conventional PID control, sliding-mode control in Filippov's sense, and relative degree concepts. The tracking of desired motion trajectories is performed in the presence of nonlinearities, modeling uncertainties, and external disturbances. The proposed methodology is successfully applied to the pitch-axis autopilot design for a tactical missile. High-level performances, robustness, and fast convergence of the closed-loop system are guaranteed.

Keywords: missile autopilot, PID controller, relative degree, robustness sliding mode control.

1. INTRODUCTION

Although the modern controllers such as LQR, LQG, H_∞ control, and μ-synthesis have been successfully applied in many areas, it has been recognized that the majority of the controllers used in control and guidance of industrial processes and engineering systems are still the Proportional-Integral-Derivative (PID) controllers. This is due to their 1-) simple structure from both mathematical and computation point of view, 2-) easy implementation, and 3-) adequate performances. However, tracking with conventional PID controllers over the operating range of highly nonlinear uncertain systems is difficult to achieve and excellent performances can not be met. In other words, for such systems conventional PID controllers lack their credibility, reliability, and robustness.

On the other hand, Variable Structure Control (VSC) has been emerged as a powerful methodology to design robust control systems and to guarantee finite time stabilization of engineering systems over their operating ranges. Using nonlinear control laws, Sliding Mode Controllers (SMCs) have been obtained with robust accommodation of modeling uncertainties, external disturbances rejection, and ability to compensate for unmodeled dynamics. Many interesting SMCs have been proposed for the guidance and control of complex systems such as aircrafts (Levant *et al.*, 2000; Chaudhuri *et al.,* 2005), spacecrafts (Wu *et al.*, 2009; Lincoln and Veres, 2010; Yeh *et al.*, 2010), and missiles (Thukral and Innocenti 1998; Zhou *et al.*, 1999; Shina *et al.*, 2006; Parkhi *et al.*, 2010; Kada, 2011).

In order to overcome the limitations of traditional PID controllers for regulation tasks and to keep the main advantages of SMCs for improved system's performances, a new methodology that combines PID control with standard sliding mode control in one approach has been recently proposed and applied to engineering systems such as DC motors (Fallahi and Azadi 2009), robots (Zhang *et al.,* 2010; Piltan 2011), and missiles (Congying *et al.*, 2008; Tang *et al.*, 2010). The obtained nonlinear-PID controllers show improved performances. But as for most of them, the design is restricted to the case for which the relative degree is equal to one, these controllers are unable to efficiently remove the chattering effect which is the main drawback of first-order SMCs (Levant 2010) and to cope with heavy modeling uncertainties.

In this paper and different from the conventional approach, a new methodology to design variable structure PID controllers is proposed. The design combines conventional PID control law with discontinuous sliding modes in Filippov's sense (Filippov 1988) to guarantee: 1-) high-level closed-loop system performance and stability objectives, 2-) robustness against modeling uncertainties and external disturbances, and 3-) chattering extinction. The discontinuous feedback control is designed based upon the relative degree concept and the system stability is proven using the Lyapunov theory. We note that the discontinuous sliding modes in Filippov's sense are largely used in the design of modern SMCs such as integral sliding modes (Defoort *et al.,* 2006) and higher-order sliding modes (Levant, 2005; Plestan *et al.,* 2007).

The remaining part of this paper is organized as follows. Section 2 states the problem and explains the proposed methodology and its design concept. Section 3 is devoted to the application of sliding-PID controllers to the design of tail-controlled missile autopilot. A nonlinear model that governs missile longitudinal dynamics and simulation results are also presented in section 3. A summary of the present work and concluding remarks are given in section 4.

2. VARIABLE STRUCTURE PID CONTROLLERS DESIGN

The selection of the sliding manifold σ, also called output constraint, is the crucial and most important step of SMCs design. The freedom in designing this manifold yields different controller structures. Generally, σ is chosen to be the tracking error $e = y - y_d$ where y is the system output and the subscript 'd' denotes the desired signal. However, relating the design of σ to the relative degree of y improves the system's performances and removes or considerably attenuates the chattering effect (Isidori 1995; Levant 2005; Kada 2011). Hence, we propose new sliding-PID structures that contain higher-order time-derivatives of the conventional tracking error. In the sequel, two sliding-PID controllers are designed, and then some structural properties of the closed-loop control, system stability, and robustness issues are discussed.

2.1 Problem statement

Consider an arbitrary minimum-phase nonlinear Single-Input-Single-Output (SISO) system subjected to different uncertainties and disturbances

$$\begin{aligned} \dot{\boldsymbol{x}} &= \boldsymbol{f}(\boldsymbol{x}) + \boldsymbol{g}(\boldsymbol{x})u + \boldsymbol{d}(\boldsymbol{x},t) \\ y &= h(\boldsymbol{x}) \end{aligned} \tag{1}$$

where $\boldsymbol{x} \in \mathbb{R}^n$ is the state vector, $u \in \mathbb{R}$ is the control input, and $y \in \mathbb{R}$ is the system output. The nonlinear mappings $\boldsymbol{f}(\boldsymbol{x}): \mathbb{R}^n \to \mathbb{R}^n$ and $\boldsymbol{g}(\boldsymbol{x}): \mathbb{R}^n \to \mathbb{R}^n$ are sufficiently smooth functions that correspond to the nominal part of the model (1). The function $h(\boldsymbol{x}): \mathbb{R}^n \to \mathbb{R}$ is a smooth continuous measurable or observable signal. The vector $\boldsymbol{d}(\boldsymbol{x},t) \in \mathbb{R}^n$ includes modeling uncertainties, unmodeled dynamics and additional perturbations such as delays, and measurement noises introduced by sensors and actuators. The system is supposed to be operated over a compact set $\mathbb{X} \subset \mathbb{R}^n$ that denotes its operating space. We now introduce some assumptions, required for the design methodology.

Assumption 1: All the states $x_i (i = 1, .., n)$ are supposed to be directly or indirectly actuated by the control input, the output y is supposed to be measurable (or observable) for all time $t > 0$ with constant and known relative degree $r > 1$ over $\mathbb{X}$, and the control input u is supposed to be bounded by some constants

$$U_{min} \le u \le U_{Max} \tag{2}$$

Assumption 2: There exists a set of known positive scalars μ_k such that the vector $\boldsymbol{f}$ and its successive time-derivatives $\boldsymbol{f}^{(k)}$ $(k = 1, \dots, r-1)$ are bounded in Euclidean norm over the set $\mathbb{X}$

$$\|\boldsymbol{f}^{(k)}\| \le \mu_k \tag{3}$$

where $\mu_k \in \mathbb{R}^+$, $\boldsymbol{f}^{(k)}$ is the k^{th} time-derivative of $\boldsymbol{f}$, and $\|\boldsymbol{v}\| = \sqrt{\boldsymbol{v}^T.\boldsymbol{v}}$ denotes the Euclidean norm of a given vector $\boldsymbol{v}$.

Assumption 3: The dynamic system (1) is operated under bounded uncertainties and disturbances. Hence, there exists a known positive scalar d_{max} such that the vectors $\boldsymbol{d}$ is bounded in Euclidean norm (i.e. $\|\boldsymbol{d}\| \le d_{max}$).

Assumption 4: The r^{th}-time derivative $y^{(r)}$ satisfies the following equation ((Isidori 1995)

$$y^{(r)} = \phi(\boldsymbol{x}) + \psi(\boldsymbol{x})u + \chi(\boldsymbol{x},t) \tag{4}$$

$$\begin{aligned} \phi(\boldsymbol{x}) &= y^{(r)}(\boldsymbol{x})\big|_{u=0} = L_f^r y(\boldsymbol{x}) \\ \psi(\boldsymbol{x}) &= \partial y^{(r)}(\boldsymbol{x})/\partial u = L_g L_f^{r-1} y(\boldsymbol{x}) \neq 0 \end{aligned} \tag{5}$$

$\chi(\boldsymbol{x},t)$ is an unknown continuous upper-bounded function.

Assumption 5: The desired output signal $y_d(t)$ is a continuous function of time and is differentiable to a necessary order equals to r. Further, it is assumed that $y_d(t)$ and its successive-time derivatives are uniformly bounded trajectories

$$\left|y_d{}^{(k)}(t)\right| \le \xi_k \quad (\xi_k \in \mathbb{R}^+, k = 0,1,\dots,r-1) \tag{6}$$

2.2 Sliding-PID controllers design

The focus is now on the design of manifolds $\sigma_r\left(e, \dot{e}, \dots, e^{(r-1)}\right)$ and controllers $u_r\left(e, \dot{e}, \dots, e^{(r-1)}\right)$ which force these manifolds to converge to zero-level and keep them on it for further time in spite of model uncertainties, external disturbances and measurement noises. Based upon the assumptions above, two manifolds are constructed using the relative degree of the tracked output, and two sliding-PID topologies are proposed as follows.

A. 1-cell feedback topology

The first sliding-PID topology is a 1-cell control scheme where an augmented PID structure that includes higher-order derivatives of the tracking error is proposed

$$\begin{aligned} \sigma_r^1\left(e, \dot{e}, \dots, e^{(r-1)}\right) = K_p e(\boldsymbol{x},t) + K_d \textstyle\sum_{k=r-1}^{1} \lambda_k L_f^k e(\boldsymbol{x},t) \\ + K_i \textstyle\int_{t_0}^{t} e(\boldsymbol{x},\tau) d\tau \end{aligned} \tag{7}$$

where σ_r^1 is supposed to be bounded continuous function, $\lambda_k \in \mathcal{R}^+$ $(k = r-1, \dots, 1)$ are design parameters, and $L_f^k(.)$ are the Lie derivatives. The following block diagram depicts the main feature of the 1-cell sliding-PID controller where the control input u is considered as a signum function of σ_r^1 given in (7).

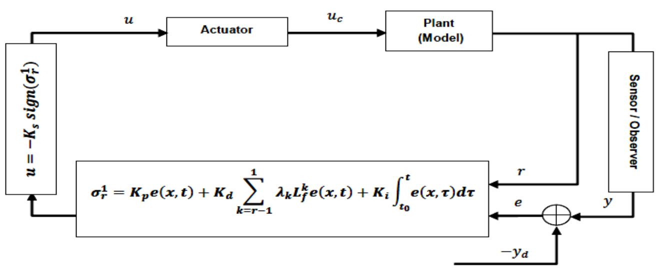

Fig. 1 Block diagram of the 1-cell sliding-PID controller

Theorem 1: *Consider the dynamic system (1) and the sliding manifold (7). If the assumptions 1-4 are fulfilled by the system dynamics and the targeted trajectory $y_d(t)$ satisfies the assumption 5, the following sliding-PID controller*

$$u_r^1 = -K_s sign\left(\sigma_r^1\left(e, \dot{e}, \dots, e^{(r-1)}\right)\right) \tag{8}$$

guarantees the convergence to zero of the manifold $\sigma_r^1\left(e, \dot{e}, \dots, e^{(r-1)}\right)$ provided that the constants K_p, K_d, K_i and the switching gain K_s are properly selected to fulfil the following gain function

$$K_s - \psi^{-1}\Big[\phi + \chi - \xi_r + (K_i + \lambda_0)(\mu_0 - \xi_0) + \left(K_p + \lambda_1\right)(\mu_1 - \xi_1) + K_d \sum_{k=r-1}^{2} \lambda_k (\mu_k - \xi_k)\Big] > 0 \tag{9}$$

(For proof see appendix A).

B. 2-cell feedback topology

The second sliding-PID topology is a 2-cell control scheme that combines a conventional PID controller with discontinuous sliding mode controller as shown in Fig 2. The sliding manifold is chosen to be a signum function

$$\sigma_r^2\left(e, \dot{e}, \dots, e^{(r-1)}\right) = \sum_{k=r-1}^{0} \lambda_k L_f^k e(\boldsymbol{x}, t) \tag{10}$$

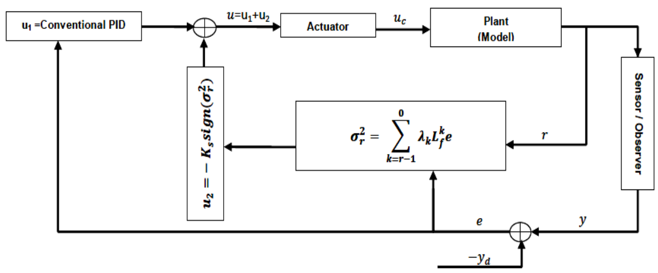

Fig. 2 Block diagram of the 2-cell sliding-PID controller

Theorem 2: *Consider that the assumptions (1)-(5) are fulfilled, for any initial state $\boldsymbol{x}_0 \in \mathbb{X}$ the following controller*

$$u_r^2 = K_p e(\boldsymbol{x}, t) + K_d \dot{e}(\boldsymbol{x}, t) + K_i \int_{t_0}^{t} e(\boldsymbol{x}, \tau) d\tau - K_s sign\left(\sigma_r^2\left(e, \dot{e}, \dots, e^{(r-1)}\right)\right) \tag{11}$$

assures that the solutions to the closed-loop system (1) converge to the attractor $\sigma_r^2 = 0$, provided that

$$K_s - K_p(\mu_0 - \xi_0) - K_d(\mu_1 - \xi_1) - K_i \upsilon + \psi^{-1}\left(\phi + \chi - \xi_r + \textstyle\sum_{k=r-1}^{1} \frac{\lambda_{k-1}}{\lambda_{r-1}}(\mu_k - \xi_k)\right) > 0 \tag{12}$$

(For proof see appendix A).

Remark 1: The controller structure (8) does not contain the conventional sliding mode equivalent control term. This means that the controller forces the system output to track the desired trajectory without reaching phase.

Remark 2: As in case of higher-order sliding mode controllers (Levant, 2005), in the absence of full system dynamics knowledge the control problem can be formulated in terms of a finite time output regulation problem (i.e. input-output stabilization problem) producing an output-feedback control.

Remark 3: In contrast to the traditional PID controllers, the proposed sliding-PID (8) and (11) completely compensate the effects of modeling uncertainties, external disturbances, and measurement noises from the beginning of the process provided that these uncertainties and disturbances are bounded.

Remark 4: The condition (5) excludes any singularity of the controllers (8) and (11).

Remark 5: The controllers (8) and (11) make the error e and its successive time-derivatives $e^{(k)}(k = 1, \dots, r-1)$ vanish in finite time.

Remark 6: The quadruplet of gains $\left(K_p, K_d, K_i, K_s\right)$ and the set of coefficients λ_k together constitute the sliding-PID design parameters. The presence of the gain K_s reduces considerably the controller parameters tuning process. Once a set of parameters λ_k and a triplet $\left(K_p, K_d, K_i\right)$ are selected, the tuning could be limited to the gain K_s only.

Remark 7: In order to smoothen the chattering effect, the signum function in the control laws (8) and (11) could be approximated within a narrow boundary layer Δ around the switching manifolds σ_r^i using saturation function (Slotine 1991) or min function or (Levant 2005).

3. SLIDING-PID CONTROLLER TO PITCH-AXIS MISSILE AUTOPILOTS

Our control objective is to design sliding-PID controllers for the pitch-axis missile dynamics such that an fast and precise tracking of a desired output is guaranteed over the operating range of the missile. For this purpose, we start this section by deriving an adequate pitch-axis missile model, and then we apply the proposed methodology to design two pitch-axis missile autopilots.

3.1 Longitudinal missile dynamics

The missile model used here is a pitch-axis model for a generic tailed-controlled missile used in many longitudinal autopilot design studies (Reichert 1992; Robert *et al.*, 1993; Xin 2008; Kada 2011).

$$\dot{M} = -K_Z M^2\left[C_{D_0} cos\alpha - C_z sin\alpha\right] - \frac{a}{v_s} sin\gamma \tag{13}$$

$$\dot{\gamma} = -K_Z M C_z cos\alpha - \frac{a}{v_s M} cos\gamma \tag{14}$$

$$\dot{\alpha} = K_Z M C_z cos\alpha + \frac{a}{v_s M} cos\gamma + q \tag{15}$$

$$\dot{q} = K_Z M^2 C_m + e_m q \tag{16}$$

where M, α, γ, and q denote the Mach number, Angle-Of-Attack (AOA), flight path angle, and pitch rate, respectively. The aerodynamic coefficients C_z and C_m are estimated from wind-tunnel measurements as follows

$$C_z = a_n\alpha^3 + b_n|\alpha|\alpha + c_n\left(2 - {}^{M}\!/_{3}\right)\alpha + d_n\delta_e \qquad (17)$$
$$C_m = a_m\alpha^3 + b_m|\alpha|\alpha + c_m\left(-7 + {}^{8M}\!/_{3}\right)\alpha + d_m\delta_e \qquad (18)$$

Description and numerical values of various aerodynamic coefficients, physical parameters, system performance requirements, and control constraints are provided in (Kada 2011). The state vector that corresponds to the model (13)-(16) is $\boldsymbol{x} = [M\ \ \gamma\ \alpha\ \ q] \in \mathbb{R}^4$, and the control input is the tail-fin deflection $u = \delta_e \in \mathbb{R}$. As the effect of the δ_e on the aerodynamic force coefficient C_z is negligible (Devaud *et al.*, 1999), the vector $\boldsymbol{g}(\boldsymbol{x})$ is reduced to

$$\boldsymbol{g}(\boldsymbol{x}) = [0 \quad 0 \quad 0 \quad K_z M^2 d_m]^T \qquad (19)$$

Since $g_4 \neq 0\ \forall\ \boldsymbol{x}$, both controllers (9) and (12) are non singular controllers over the operating range of the missile.

3.2 Pitch-axis autopilot design

It is shown in the previous section that the controller topologies are related to the influence of the control input on the dynamics of the tracking variable, and to the relative degree of this variable. Considering the case of $\boldsymbol{y} = \boldsymbol{x}$, the relative degree vector is equal to $\boldsymbol{r} = [3\ 3\ 2\ 1]$. All the states in the model (13)-(16) are measurable or observable functions.

A. AOA sliding-PID Autopilots

With relative degree $r_\alpha = 2$ and tracking error $e = (\alpha - \alpha_d)$, we find

$$\sigma_2^1 = K_p(\alpha - \alpha_d) + K_d\lambda_1(\dot{\alpha} - \dot{\alpha}_d) + K_i\int_{t_0}^{t}(\alpha - \alpha_d)d\tau \qquad (20)$$
$$\sigma_2^2 = \lambda_1(\dot{\alpha} - \dot{\alpha}_d) + \lambda_0(\alpha - \alpha_d) \qquad (21)$$

In order to evaluate the performance, efficiency, and agility of the controllers (8) and (11), the missile is subjected to periodic and sudden change in commands in terms of AOA patterns as shown in Fig. (3).

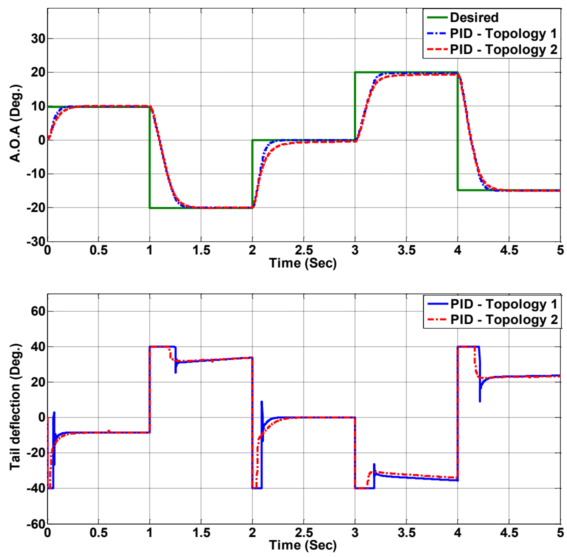

(a)

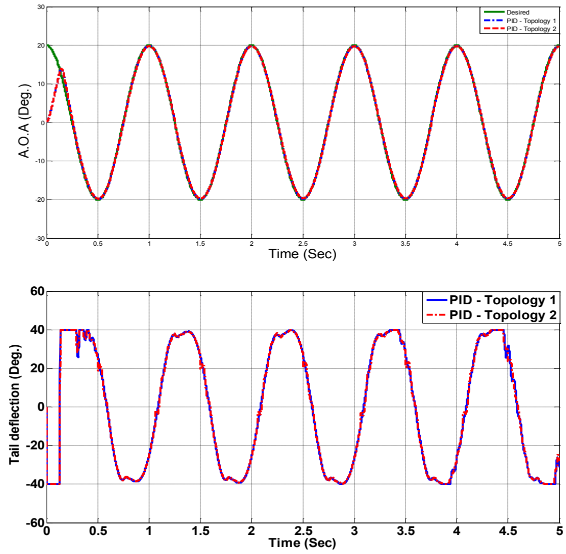

(b)

Fig. 3. Time history responses and tail-fin deflections corresponding to desired A.O.A paths: (a) path with sudden changes, (b) sinusoidal path.

During the gain-tuning procedure, we have found that the controller (8) is more flexible than the controller (11).

B. Velocity-hold sliding-PID Autopilots

Both Mach number M and path angle γ have a relative degree $r = 3$. In many missile autopilot designs the output M is used as speed tracking variable. In this case and with $e = (M - M_d)$, the dynamics of the sliding manifold (7) is given by

$$\sigma_1^2 = K_p(M - M_d) + K_d\lambda_2(\ddot{M} - \ddot{M}_d) + K_d\lambda_1(\dot{M} - \dot{M}_d) + K_i\int_{t_0}^{t}(M - M_d)d\tau \qquad (22)$$

In this scenario, the system is forced to maintain a desired velocity for long a certain period of time with presence of modelling uncertainties in aerodynamic coefficients a-) 75% under and overestimation, and b-) sinusoidal variation of the form

$$C_i = C_{i,0}(1 + k\cos(w_0 t)) \qquad (23)$$

where C_i is an aerodynamic coefficient, $C_{i,0}$ is the nominal value of C_i, and k, w_0 are constants.

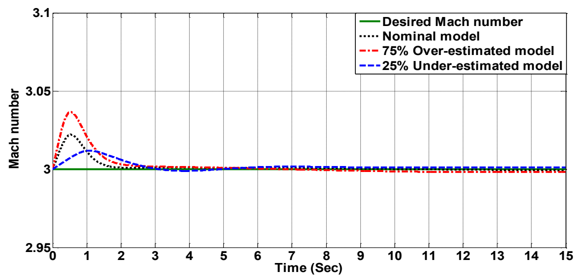

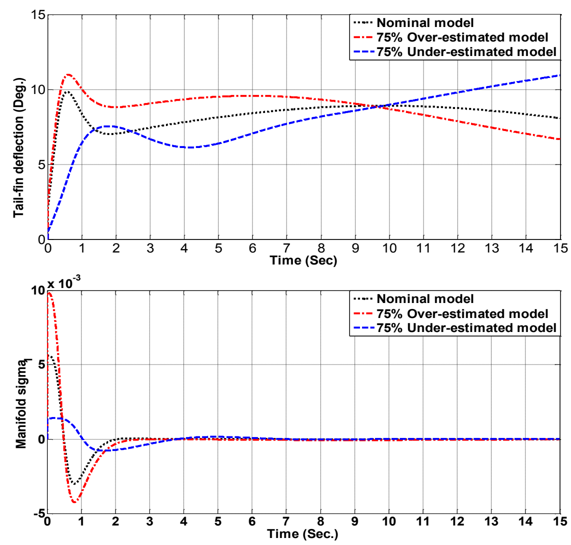

(a)

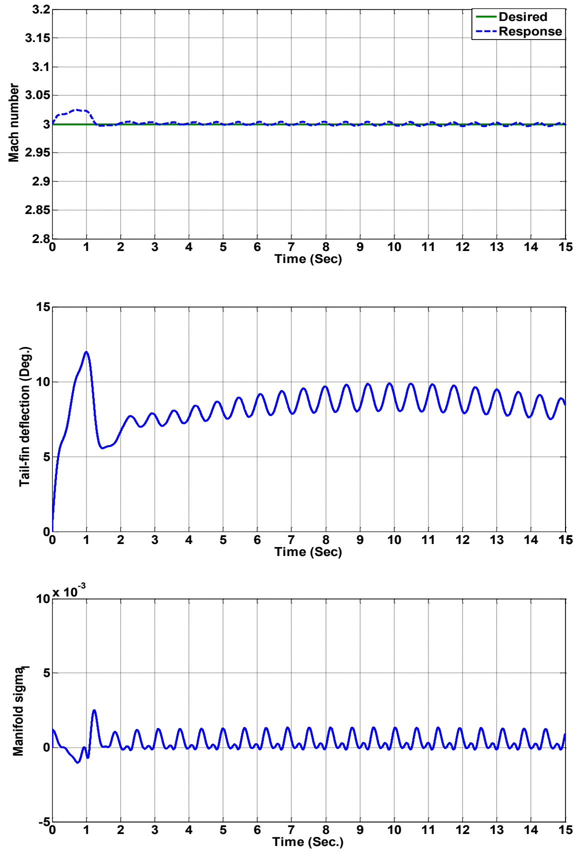

(b)

Fig. 4. Mach number, tail-fin deflection, and sliding manifold corresponding to a velocity-hold command: (a) modeling parameter variations, (b) sinusoidal variation of parameters.

We note that all the simulation scenarios were run in Matlab environment.

4. CONCLUSION

In this paper, a new methodology to design sliding-PID controllers that assure consistent performances and present high robustness and abilities to cope with uncertainty and disturbance conditions has been proposed. Computer simulations proved that the designed sliding-PID controllers for missile pitch-axis autopilot achieve robust performance and stability in the presence of bounded modeling uncertainties. Both controllers assured fast convergence with chattering free sliding mode characteristics. With such motion tracking capabilities, the proposed control methodology promises the realization of high-performance robust controllers.

REFERENCES

Chaudhuri, A. and B. M. S. Bhat (2005). Output feedback-based discrete-time sliding-mode controller design for model aircraft. *Journal of guidance control and dynamics*, volume (28), pages 177-181.

Congying, L., Shixing, W., Zhi, Y.e, Jinygon, Y. and Huijin, W. (2008). Anti-windup nonlinear PID controller design and its application to winged missile control system. *Proceedings of the 27th Chinese control conference*, pages 377-379.

Defoort, M., Floquet, T., Kokosy, A. and Perruquetti, W. (2006). Finite-time control of a class of MIMO nonlinear systems using high order integral sliding mode control. *Proceeding of the international workshop on variable structure systems*, pages 133-138.

Devaut, E., Hiret, A. and Siguerdidjane, H. (1999). Dynamic inversion and LPV approach: application to a missile autopilot. *In proceedings of the IEEE Hong-Kong symposium on robotics and control*, volume (1), pages 293-298.

Fallahi, M. and Azadi, S. (2009). Fuzzy PID sliding mode controller design for the position control of a DC motor. *In proceeding ICETC*, pages73-77.

Filippov, A.F. (1988). *Differential equation with discontinuous right-hand sides*. Kluwer Academic Publishers, Dordrecht (Netherlands), Boston.

Isidori, A. (1995). *Nonlinear control systems*. Springer-Verlag. Berlin and others, 3rd edition.

Kada, B. (2011). Outer-loop sliding mode control approach to longitudinal autopilot missile design. *IFAC 18th world congress*, volume (18), part I, pages 11147-11164.

Levant, A., Pridor, A., Ben-Asher, J.Z., Gitizadeh, R., and Yaesh, I. (2000). 2-sliding mode implementation in aircraft pitch control. *Journal of guidance control and dynamics*, volume (23), pages 586-594.

Levant, A. (2005). Homogeneity approach to high-order sliding mode design. *Automatica*, volume (41), pages 823-830.

Levant, A. (2010). Chattering Analysis. *IEEE transactions on automatic control*, volume (55), no 6, pages 1380-1389.

Lincoln, N. K. and Veres, S.M. (2010). Application of discrete time sliding mode control to a spacecraft in 6DoF. *International journal of control*, volume (83) no 9, pages1-10.

Parkhi, P., Bandyopadhyay, B. and Jha, M. (2010). Design of roll autopilot for a tail controlled missile using sliding mode technique. *11th international workshop on variable structure systems*. pages 389 – 394.

Piltan, F., Sulaiman, N., Gavahian, A., Soltani, S. and Roosta, S. (2011). Design mathematical tunable gain PID-like sliding mode fuzzy controller with minimum rule base. *Journal of robotics and automation,* volume (2) Issue 3, pages 146-156.

Plestan, F., Glumineau, A. and Laghrouche, S. (2007). A new algorithm for higher-order sliding mode control. *Journal of robust nonlinear control*. volume (18), pages 441-453.

Reichert, R.T. (1992). Dynamic scheduling of modern robust-control autopilot design for missiles. *IEEE control systems,* magazine (12) no 5, pages 35-42.

Robert, A., Reichert, T.R. and Rugh, J. (1993). Gain scheduling for H-infinity controllers: a flight control example. *IEEE transactions on control systems technology*, volume (1) no 2, pages 69-79.

Shina, T., Idan, M. and Golan, O.M. (2006). Sliding-mode control for integrated missile autopilot guidance. *Journal of guidance, control, and dynamic, volume (29) no.2,* pages250-260.

Slotine, J.E. and Li, W. (1991). *Applied nonlinear control.* Prentice-Hall Inc., London.

Tang, J., Hu, Y., Xiao, Z. and Li, J. (2010). Missile PID controller parameter tuning based on iterative learning control. *2nd international conference on signal processing systems,* volume (3). pages 689-692.

Thukral, A. and Innocenti, M. (1998). A sliding mode missile pitch autopilot synthesis for high angle of attack maneuvering. *IEEE transactions on control systems technology*, volume (6) issue 3, pages 359-371.

Wu, Z., Sun, Z. and Li, H. (2009). Sliding mode controller design for rigid satellite attitude tracking. *International conference on robotics and biomimetics,* pages 2238-2243.

Yeh, F.-K. (2010). Sliding-mode adaptive attitude controller design for spacecrafts with thrusters. *IET control theory application*, volume (4) issue 7, pages 1254–1264.

Zhang, D.L., Chen, Y.P., Xie, J.M., Ai, W. and Yuan, C.M. (2010). A hybrid control method of sliding mode and PID controllers based on adaptive controlled switching portion. *Proceedings of the 29th Chinese control conference,* pages 439-445.

Zhou, D, Chundi, M. and Wenli, X. (1999). Adaptive sliding-mode guidance of a homing missile. *Journal of guidance, control, and dynamics*, volume (22) no. 4, pages 589-594.

Appendix A

The variable structure controllers (8) and (11) are constructed such that the η-reaching condition ($\sigma\dot{\sigma} < -\eta|\sigma|$) is fulfilled with $\eta \in \mathbb{R} > 0$. Assuming that the system (1) is known, the full state is available (i.e., all the states are measurable or observable variables) and the output $y = x_i (i = 1, \dots, n)$, the theorems 1 and 2 are proven as follows.

A.1 Proof of theorem 1

From (7), the time-derivative of σ_r^1 is defined as

$$\dot{\sigma}_r^1 = y^{(r)}(\boldsymbol{x},t) - y_d^{(r)}(t) + (K_i + \lambda_0)\, e(\boldsymbol{x},t) + \left(K_p + \lambda_1\right) \dot{e}(\boldsymbol{x},t) + K_d \textstyle\sum_{k=r-1}^{2} \lambda_k e^{(k)}(\boldsymbol{x},t) \quad (24)$$

Using (4) we write

$$\dot{\sigma}_r^1 = \phi(\boldsymbol{x}) + \psi(\boldsymbol{x})u + \chi(\boldsymbol{x},t) - y_d^{(r)}(t) + \varphi_1(e) \quad (25)$$

with

$$\varphi_1(e) = (K_i + \lambda_0)\, e(\boldsymbol{x},t) + \left(K_p + \lambda_1\right) \dot{e}(\boldsymbol{x},t) + K_d \textstyle\sum_{k=r-1}^{2} \lambda_k\, e^{(k)}(\boldsymbol{x},t) \quad (26)$$

If $\sigma_r^1 \neq 0$, the stability of the system is checked as follows

$$\begin{aligned}
\dot{V}(\boldsymbol{x},t) &= \sigma_r^1 \dot{\sigma}_r^1 \\
&= \sigma_r^1\left[\phi + \psi u + \chi - y_d^{(r)} + \varphi_1(e)\right] \\
&= \sigma_r^1\left[\phi - \psi K_s sign(\sigma_r^1) + \chi - y_d^{(r)} + \varphi_1(e)\right] \\
&\leq -|\sigma_r^1||\psi|\left[K_s - \psi^{-1}\left(\phi + \chi - y_d^{(r)} + \varphi_1(e)\right)\right] \\
&\leq -|\sigma_r^1|\psi_{max}\big[K_s - \psi^{-1}[\phi + \chi - \xi_r + (K_i + \lambda_0)\,(\mu_0 - \xi_0) \\
&\quad + \left(K_p + \lambda_1\right)(\mu_1 - \xi_1) + K_d \textstyle\sum_{k=r-1}^{2} \lambda_k\,(\mu_k - \xi_k)]\big] \\
&< -\eta|\sigma_r^1|
\end{aligned} \quad (27)$$

provided that

$$K_s - \psi^{-1}\Big[\phi + \chi - \xi_r + (K_i + \lambda_0)\,(\mu_0 - \xi_0) + \left(K_p + \lambda_1\right)(\mu_1 - \xi_1) + K_d \sum_{k=r-1}^{2} \lambda_k\,(\mu_k - \xi_k)\Big] > 0 \quad (28)$$

A.2 Proof of theorem 2

From (10) and (4), the time-derivative of σ_r^2 is found to be

$$\dot{\sigma}_r^2 = \lambda_{r-1}\left(\phi(\boldsymbol{x}) + \psi(\boldsymbol{x})u + \chi - y_d^{(r)}(t)\right) + \varphi_2(e) \quad (29)$$

with $\varphi_2(e) = \sum_{k=r-1}^{1} \frac{\lambda_{k-1}}{\lambda_{r-1}} e^{(k)}$ (30)

If $\sigma_r^2 \neq 0$ and $\int_{t_0}^{t} e(\boldsymbol{x},\tau)d\tau \leq \upsilon \in \mathbb{R}$, we find

$$\begin{aligned}
\dot{V}(\boldsymbol{x},t) &= \sigma_r^2 \dot{\sigma}_r^2 \\
&= \sigma_r^2 \lambda_{r-1}\left[\phi + \psi u + \chi - y_d^{(r)} + \varphi_2(e)\right] \\
&= \sigma_r^2 \lambda_{r-1}\left[\phi + \psi\left(u_{PID} - K_s sign(\sigma_r^2)\right) + \chi - y_d^{(r)} + \varphi_2(e)\right] \\
&\leq -|\sigma_r^2|\lambda_{r-1}|\psi|\left[K_s - u_{PID} - \psi^{-1}\left(\phi + \chi - y_d^{(r)}\right) + \varphi_2(e)\right] \\
&\leq -|\sigma_r^2|\lambda_{r-1}\psi_{max}\Big[K_s - K_p\,(\mu_0 - \xi_0) - K_d\,(\mu_1 - \xi_1) \\
&\quad - K_i\,\upsilon + \psi^{-1}\left(\phi + \chi - \xi_r + \textstyle\sum_{k=r-1}^{1} \frac{\lambda_{k-1}}{\lambda_{r-1}}(\mu_k - \xi_k)\right)\Big] \\
&< -\eta|\sigma_r^2|
\end{aligned} \quad (31)$$

provided that

$$K_s - K_p\,(\mu_0 - \xi_0) - K_d\,(\mu_1 - \xi_1) - K_i\,\upsilon + \psi^{-1}\left(\phi + \chi - \xi_r + \textstyle\sum_{k=r-1}^{1} \frac{\lambda_{k-1}}{\lambda_{r-1}}(\mu_k - \xi_k)\right) > 0 \quad (32)$$